

KEY RESULTS FROM IRRADIATION AND POST-IRRADIATION EXAMINATION OF AGR- 1 UCO TRISO FUEL

2016 International Topical Meeting on High
Temperature Reactor Technology (2016)

Paul A. Demkowicz, John D. Hunn,
David A. Petti, Robert N. Morris

November 2016

The INL is a
U.S. Department of Energy
National Laboratory
operated by
Battelle Energy Alliance



This is a preprint of a paper intended for publication in a journal or proceedings. Since changes may be made before publication, this preprint should not be cited or reproduced without permission of the author. This document was prepared as an account of work sponsored by an agency of the United States Government. Neither the United States Government nor any agency thereof, or any of their employees, makes any warranty, expressed or implied, or assumes any legal liability or responsibility for any third party's use, or the results of such use, of any information, apparatus, product or process disclosed in this report, or represents that its use by such third party would not infringe privately owned rights. The views expressed in this paper are not necessarily those of the United States Government or the sponsoring agency.

KEY RESULTS FROM IRRADIATION AND POST-IRRADIATION EXAMINATION OF AGR-1 UCO TRISO FUEL

Paul A. Demkowicz¹, John D. Hunn², David A. Petti¹, Robert N. Morris²

¹ Idaho National Laboratory, P.O. Box 1625, Idaho Falls ID 83415-6188, USA

² Oak Ridge National Laboratory, P.O. Box 2008, Oak Ridge TN, 37831-6093, USA

Corresponding author: paul.demkowicz@inl.gov, +1-208-526-3846

The AGR-1 irradiation experiment was performed as the first test of tristructural isotropic (TRISO) fuel in the US Advanced Gas Reactor Fuel Development and Qualification Program. The experiment consisted of 72 right cylinder fuel compacts containing approximately 3×10^5 coated fuel particles with uranium oxide/uranium carbide (UCO) fuel kernels. The fuel was irradiated in the Advanced Test Reactor for a total of 620 effective full power days. Fuel burnup ranged from 11.3 to 19.6% fissions per initial metal atom and time average, volume average irradiation temperatures of the individual compacts ranged from 955 to 1136°C. This paper focuses on key results from the irradiation and post-irradiation examination, which revealed a robust fuel with excellent performance characteristics under the conditions tested and have significantly improved the understanding of UCO coated particle fuel irradiation behavior. The fuel exhibited zero TRISO coating failures (failure of all three dense coating layers) during irradiation and post-irradiation safety testing at temperatures up to 1700°C. Advanced PIE methods have allowed particles with SiC coating failure that were discovered to be present in a very low population to be isolated and meticulously examined, which has elucidated the specific causes of SiC failure in these specimens. The level of fission product release from the fuel during irradiation and post-irradiation safety testing has been studied in detail. Results indicated very low release of krypton and cesium through intact SiC and modest release of europium and strontium, while also confirming the potential for significant silver release through the coatings depending on irradiation conditions. Focused study of fission products within the coating layers of irradiated particles down to nanometer length scales has provided new insights into fission product transport through the coating layers and the role various fission products may have on coating integrity. The broader implications of these results and the application of lessons learned from AGR-1 to fuel fabrication and post-irradiation examination for subsequent fuel irradiation experiments as part of the US fuel program are also discussed.

I. INTRODUCTION

The AGR-1 irradiation experiment was designed as the initial performance test of tristructural isotropic (TRISO) fuel fabricated at the laboratory scale in the US, and was the first step in the progression of fuel fabrication from the laboratory to an industrial vendor.¹ It also served as a shake-down test for test train design, irradiation methodology, and post-irradiation examination methods, and has provided invaluable early data on fuel performance.

The AGR-1 fuel kernels were a heterogeneous mixture of uranium oxide and uranium carbide (termed UCO) with 19.74% U-235 enrichment and were fabricated at BWX Technologies Nuclear Operations Group. The TRISO coatings were applied at Oak Ridge National Laboratory (ORNL) and had nominal thicknesses of 100 µm for the porous carbon buffer, 40 µm for the inner pyrolytic carbon (IPyC) layer, 35 µm for the SiC layer, and 40 µm for the outer pyrolytic carbon (OPyC) layer. The coated particles were formed into right cylindrical compacts at ORNL that were nominally 12.4 mm in diameter and 25.1 mm in length. Compacts contained approximately 4,100 particles with a packing fraction of approximately 37%.^{2,3}

A baseline fuel and three different fuel variants were fabricated. Fabrication of each variant involved modification of the deposition conditions and properties of either the inner pyrolytic carbon (IPyC) or SiC layer relative to the Baseline in order to explore the effect of various coating properties on irradiation performance.^{4,5} For Variant 1, the IPyC coating layer conditions were varied to provide a slightly lower anisotropy and density. For Variant 3, the SiC layer deposition conditions were varied to provide a finer grain microstructure relative to the Baseline fuel. Specifically, the SiC deposition temperature was decreased for the Variant 3 fuel from 1500 to 1425°C and argon was added as a diluent to the hydrogen carrier gas. Details on the fuel fabrication parameters and observations of the Baseline and Variant 3 SiC microstructures are provided in Refs. 4 and 6. Fabrication of the different fuel types also resulted in minor differences in other average properties (including coating thickness,

number of particles per compact, packing fraction, and defect populations).⁷

The irradiation experiment consisted of six separate capsules, each with independent sweep gas flow and temperature monitoring and control. Each capsule contained 12 fuel compacts of a single fuel type retained in a graphite fuel holder in three stacks oriented in a triangular array (Fig. 1), with each stack containing four compacts.⁸

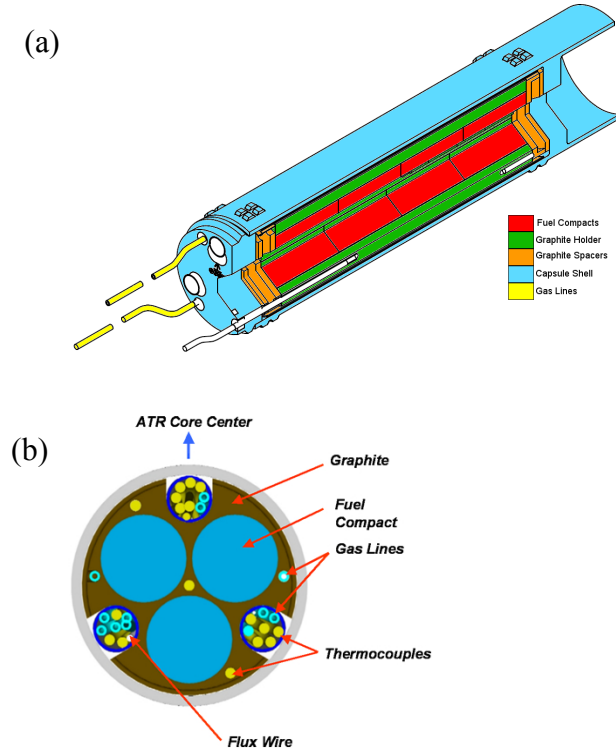


Fig. 1. Cutaway diagram of an AGR-1 capsule showing the key components (a) and cross-sectional view of a capsule (b).

The irradiation was performed from December 2006 to November 2009 in the Advanced Test Reactor at Idaho National Laboratory (INL) for a total of 620 effective full power days. The calculated compact average burnup ranged from 11.3 to 19.6% fissions per initial metal atom (FIMA), and compact average fast neutron fluence ($E > 0.18$ MeV) ranged from 2.17 to 4.30×10^{25} n/m². The time-average, volume-average (TAVA) compact temperatures were 955–1136°C and the time-average maximum compact temperatures were 1069–1197°C. Based on the low fission gas release-to-birth ratios in all of the capsules, there were zero TRISO-coating failures during the irradiation out of a total of approximately 3×10^5 particles in the experiment.^{8,9}

Post-irradiation examination (PIE) and safety testing of the AGR-1 fuel commenced in 2010 at INL and ORNL.

The PIE was focused on evaluating fuel performance during irradiation and during post-irradiation high temperature heating tests in helium. Key aspects of fuel performance that were investigated were fission product release from particles and compacts, and radiation-induced changes in kernel and coating microstructures. Safety tests were performed by heating the fuel compacts in helium at temperatures of 1600, 1700, or 1800°C, with nominal hold times of 300 h.¹⁰ The PIE and safety results have been discussed in detail previously, and the results are summarized in Ref. 11. This paper will highlight some of the key findings from the PIE and safety testing in terms of UCO fuel performance.

II. FISSION PRODUCT RELEASE

Extensive data were obtained on the release of fission products during the irradiation and during post-irradiation heating tests. This includes data on release from individual particles, retention in the compact matrix, and overall release from fuel compacts. A brief summary of the results for key elements is provided here.

II.A. Krypton

Fission gas release during the irradiation was generally very low. Release-to-birth ratios for short-lived fission gases Kr-85m, Kr-88, and Xe-135 were well below 10^{-7} for most of the irradiation, while values as high as 2×10^{-7} were observed in one of the six capsules near the end of irradiation.⁹ These low values (less than 0.1% of the inventory in a single particle) indicate that no TRISO particles failed during the irradiation in any of the capsules, which each contained approximately 5×10^4 particles.

During safety testing, eight compacts were heated at 1600°C and three compacts were heated at 1700°C, with no observed TRISO failures and very low Kr-85 release. Compact Kr-85 release fractions were all below 6×10^{-6} (1600°C) or 10^{-5} (1700°C) during these tests. Increasing the test temperature to 1800°C (four compacts tested) resulted in greater krypton release. In one test, the data clearly indicate that two particles experienced TRISO failure after more than 200 h at 1800°C, and as a result, the Kr-85 release fraction reached approximately 5×10^{-4} .^{10,12} In the other three 1800°C tests, no TRISO failures were evident and Kr-85 peaked at 6×10^{-5} . The higher release compared to the 1600 and 1700°C tests is primarily due to a greater number of particles that experienced SiC failure (discussed further below) and the higher temperature allowing increased diffusion of krypton through the OPyC, which was the last remaining intact TRISO layer.

II.B. Silver

Data on silver release during the AGR-1 irradiation were collected from several methods.^{11,13} The Ag-110m

inventory was measured on the empty capsule components to determine the total release from the twelve compacts in each capsule, providing a capsule-average release fraction when compared to the calculated inventory. Individual compacts were also gamma-scanned to quantify the inventory of Ag-110m remaining, allowing a release fraction to be estimated for each compact. Finally, individual particles from a select number of compacts were gamma counted to determine the inventory remaining, allowing a release fraction to be estimated for the particles. Note that in all cases, the measured inventory was compared to predicted values from physics simulations (with appropriate correction for post-irradiation decay), and therefore the calculated release fractions are subject to uncertainty or bias in the predicted inventory, estimated to be approximately $\leq 15\%$.

Table 1 shows the range of Ag-110m release fractions determined using each approach. The results confirm that silver release can be very high, depending on irradiation conditions and the sample size. When considering capsule-average release from the compacts, values ranged from 0.012 to 0.38, and tended to increase with capsule temperature. However, looking at individual compacts, silver release ranged from very low values to as high as approximately 92%. In the case of individual particles, values could range from essentially complete retention to complete release, often with very high variability within a single compact.¹³

Table 1. Summary of AGR-1 Ag-110m release fractions

Basis	Ag-110m release fractions
Capsule average compact release	0.012 – 0.38
Individual compact release	~ 0 – 0.92
Individual particle release	~ 0 – 1.0

During safety testing of the fuel compacts, it was found that regardless of test temperature, there was an initial, rapid release of relatively large amounts of Ag-110m, either during the ramp to the target temperature, or within a short time after reaching the target temperature (Fig. 2). Based on the observed behavior during safety tests, destructive examination of as-irradiated compacts, and destructive examination of compacts after safety tests, it was concluded that this initial release was due primarily to inventory that resided in the compact matrix at the end of the irradiation, but was rapidly released during the heating test.

Little significant additional release was normally observed for the duration of the heating tests (Fig. 2). The

exception to this behavior was that of the two Variant 3 compacts heated at 1800°C. It was observed that after approximately 100 h at 1800°C, the silver release rate began to increase (see the two data sets in red Fig. 2 which exhibit increased silver release after ~ 100 h). This behavior was consistent for both Variant 3 compacts, but was not observed for the Baseline and Variant 1 compacts heated at the same temperature, both of which had a similar SiC microstructure with larger grains relative to Variant 3.⁶ The conclusion is that the smaller-grain SiC apparently allows more rapid diffusion of silver after extended times at this extreme temperature.¹⁰ An additional test performed on individual Variant 3 particles heated to 1800°C also showed silver release rates similar to those observed in the two Variant 3 compacts, with most particles retaining no detectable Ag-110m after 650 h.¹⁴

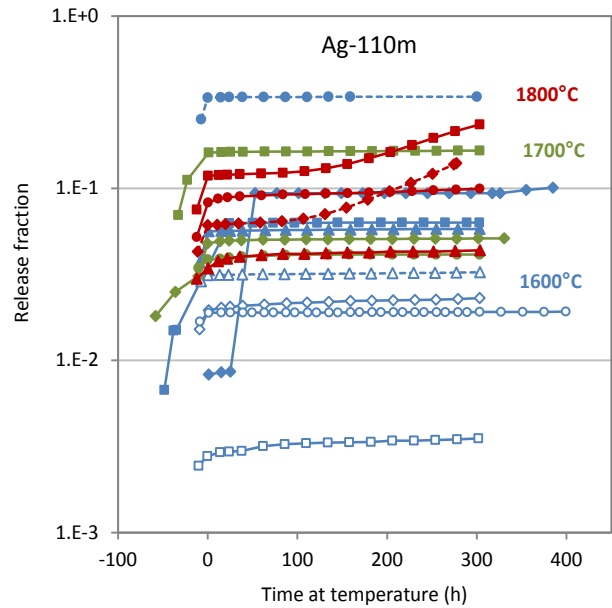


Fig. 2. Ag-110m fractional release from AGR-1 compacts during safety tests. Test temperature is indicated by the color coding shown in the figure. Note the increase in release fraction for two of the 1800°C tests (in red) after ~ 100 h at 1800°C.

The results confirmed previous observations regarding silver release from TRISO fuel dating back several decades; in particular, that silver release can be quite high depending on irradiation conditions.^{15,16} The results also indicated that silver release may exhibit some unusual temperature dependence (details can be found in Ref. 11). Because of a relatively large variation in fuel temperatures within a given capsule as a function of time,¹⁷ many of the AGR-1 fuel compacts spent significant portions of the irradiation at temperatures well above the reported TAVA temperatures, and these high temperatures were likely a contributing factor in some of the high silver release values

observed. As an example, Compact 6-2-3 (overall TAVA temperature of 1136°C), which is estimated to have lost in excess of 90% of the predicted Ag-110m inventory, was calculated to have had a volume-average temperature greater than 1300°C for over 80 days.

II.C. Cesium

A key finding from the AGR-1 PIE and safety testing was that cesium release was heavily dependent on discrete failures of the SiC layer, and that release through otherwise intact SiC was very low, even at temperatures as high as 1800°C. This finding was made possible by the ability to locate and perform detailed characterization on the small number of particles that experienced SiC failure, both during irradiation and during post-irradiation safety testing (discussed in detail in Ref. 18 and summarized in Section IV). An important distinction is that cesium release did not appear to gradually increase from particles due to a slow degradation of the SiC layer with corresponding gradual increase in transport through the layer during safety tests, but rather a significant fraction of cesium would be released from a particle in a relatively short time period upon loss of retentivity by the SiC layer.

In four of the six irradiation capsules, the total compact-average cesium release fraction during the irradiation was $<3 \times 10^{-6}$ (likely much lower, but the actual levels were difficult to quantify due to the inability to detect cesium on some of the capsule components¹⁹). In the other two capsules, compact average release fractions were around 10^{-5} . In the latter case, the primary cause of the cesium release was found to be a small number of particles which experienced SiC failure and released a significant fraction of their expected inventory.^{11,18}

During safety testing, compact Cs-134 release fractions were $<5 \times 10^{-6}$ if all SiC layers remained intact.¹⁰ This was true in one case even at 1800°C for ~ 100 h, after which a SiC layer failure occurred with corresponding cesium release. On the other hand, compacts in which one or more particles experienced SiC layer failure exhibited Cs-134 releases that rapidly reached a level of 10^{-4} or greater. This Cs-134 release behavior during safety tests is summarized in Fig. 3. Note the two distinct populations: compacts with final test release $<5 \times 10^{-6}$ and those $>10^{-4}$ (the fraction equivalent to a single particle inventory in these compacts is 2.4×10^{-4}). The presence of SiC failures in the latter population was confirmed by extensive destructive examination of the compacts after the tests, including gamma counting of each individual particle to locate those with low cesium inventory and x-ray tomography to identify SiC degradation in these particles.¹⁸ Overall, Cs-134 release from the compacts was $\leq 2 \times 10^{-4}$ after 300 h at 1600°C, and about an order of magnitude higher after 300 h at 1800°C.

The obvious implication of the AGR-1 results is that the overall cesium release from the fuel is strongly related

to the number of discrete SiC failures that occur. The cause of SiC layer failures in the AGR-1 fuel was studied in detail (Section IV). While cesium release of similar or higher levels has been observed previously with irradiated UO₂ fuel,²⁰⁻²² the nature of the SiC layer failures in specific particles has not been explored in detail. It is possible that the general method of SiC layer failure is appreciably different in UCO fuel compared to UO₂ fuel, where degradation of the SiC layer by reaction with CO may be a major contributing factor. PIE and safety testing of fuel from the AGR-2 irradiation experiment (which included both UCO and UO₂ fuel forms) is currently in progress,^{23,24} and may provide a better understanding of these differences.

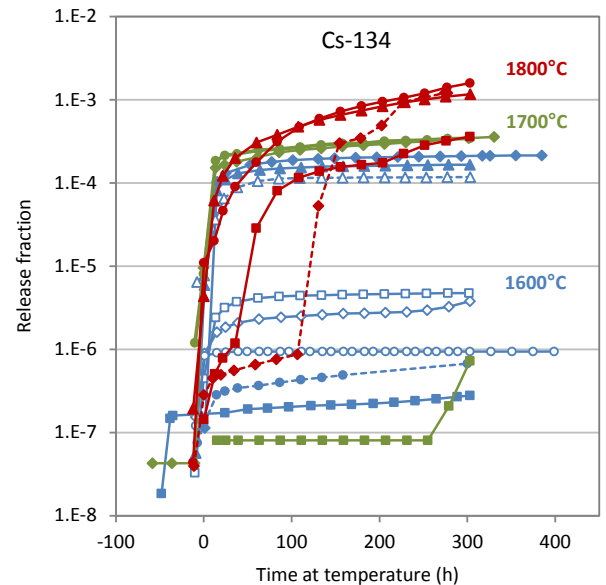


Fig. 3. Cs-134 fractional release from AGR-1 compacts during heating tests. Test temperature is indicated by the color coding shown in the figure.

II.D. Europium and Strontium

Europium and strontium release behavior was relatively similar. In both cases, the data indicate a modest amount of release from the particles through intact SiC during irradiation. The amount of release was assessed by two means: measurement of the inventory in the compact matrix of irradiated compacts (which provides the inventory released from particles but retained within the compact) and measurement of the inventory on the capsule components (which provides the total release from all 12 compacts in each capsule).¹¹ Fig. 4 summarizes the results from these two sets of measurements for both Eu-154 and Sr-90. The data labeled “compacts” represents the range of inventory fractions found in the matrix of nine compacts destructively examined. Data labeled “capsules” is the range of values (expressed as the fraction of the total

capsule inventory) released from compacts in the six irradiation capsules. The fraction corresponding to the inventory of a single particle is shown for both compacts (2.4×10^{-4}) and entire capsules (2.0×10^{-5}).

Europium release was on average higher than strontium. In both cases, a significant fraction of the inventory released from particles was retained in the matrix, rather than being released from the compact. The maximum release from the compacts was 5×10^{-4} for Eu-154, and 3×10^{-5} for Sr-90.

During safety testing at 1600 and 1700°C, the release rates of both europium and strontium from individual compacts remained relatively constant for the duration of the 300 h tests.¹⁰ It appears that the majority of the release during these tests was due to inventory that was in the matrix at the end of the irradiation, which was gradually released at higher temperatures during safety tests. At 1800°C, it appears that additional release from the intact particles may have started to contribute appreciably.

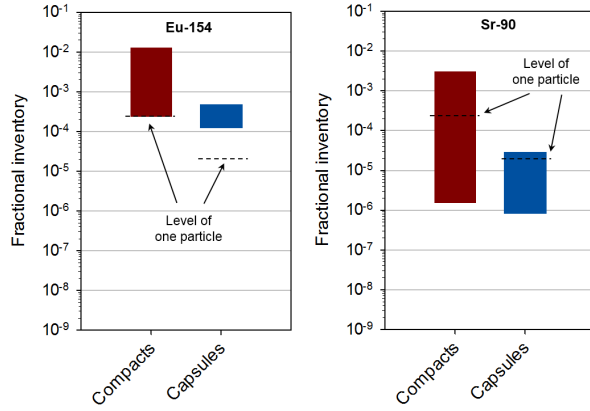


Fig. 4. Data on Eu-154 and Sr-90 release from the AGR-1 fuel. Data labeled “compacts” represents inventory in the compact matrix after irradiation. Data labeled “capsules” represents the total inventory fraction released from compacts in each of the six capsules.

III. IRRADIATED PARTICLE MICROSTRUCTURE EVOLUTION

Extensive microscopic examination of particle cross-sections was performed. This included numerous cross-sections of select intact as-irradiated compacts²⁵ as well as loose particles deconsolidated from numerous as-irradiated or safety-tested compacts. Common features in the irradiated particles included densification of the buffer layer and swelling of the kernel with related formation of gas-filled bubbles (Fig. 5). There was no detectable high-burnup kernel migration (the so-called “amoeba effect”), indicating the efficacy of the UCO fuel in limiting the oxygen partial pressure in the fuel and the formation of carbon monoxide.

In the majority of particles, the buffer layer debonded from the IPyC layer. This was observed as either complete (Fig. 5a) or partial (Fig. 5b) debonding in the polished plane analyzed. Much less common were particles in which the buffer and IPyC layers remained completely bonded in the plane observed (Fig. 5c), where the buffer densification resulted in the inner diameter increasing while the kernel swelled to filled the increasing volume. Such particles constituted 4% of approximately 1,000 particles observed in a study of compact cross sections.²⁵

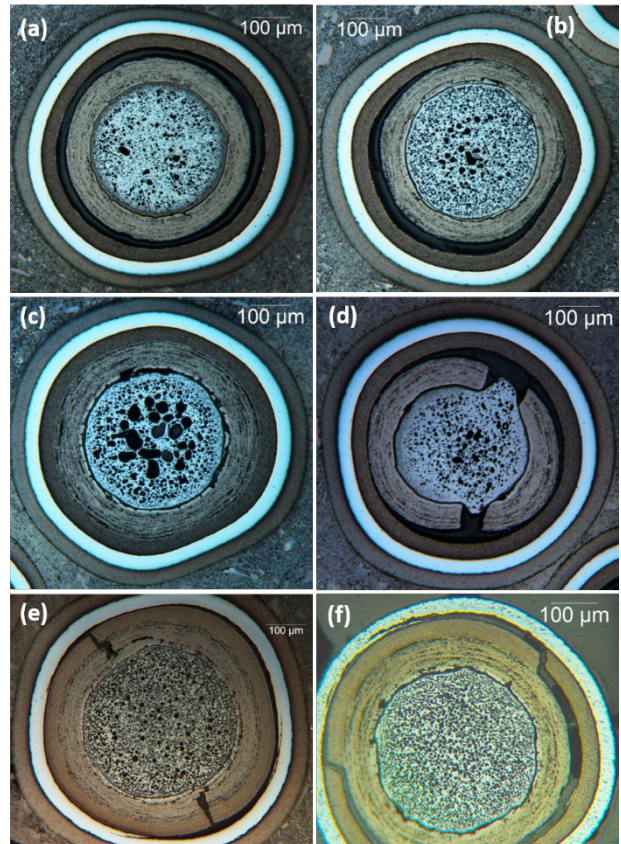


Fig. 5. Examples of various AGR-1 irradiated particle microstructures (from Ref. 25).

Fracture of the buffer layer was not uncommon (observed in 23% of particles studied in the compact cross sections discussed in Ref. 25), and these were often accompanied by expansion of the kernel into the gap formed at the point of fracture (Fig. 5d). While particles with the representative microstructure shown in Fig. 5d were fairly common, there appeared to be no obvious detrimental effects on the outer, dense coating layers, even in cases where the kernel was in direct contact with the IPyC layer. On the other hand, if the buffer-IPyC interface remained intact as in Fig. 5c, fracture of the buffer layer was always accompanied by fracture of the IPyC layer, and often also included debonding of the IPyC from the SiC layer (Fig. 5e).

Fracture of the buffer layer was not always necessary for IPyC fracture to occur. In some particles, partial debonding of the buffer-IPyC layer apparently led to development of sufficient stress in the IPyC layer to cause fracture (Fig. 5f), often with resultant debonding between the IPyC and SiC layers and in rare cases, partial fracture of the SiC at the IPyC-SiC interface (as shown in Fig. 5f) that did not lead to SiC failure. Because partial buffer-IPyC debonding (Fig. 5b) was much more common than no debonding (Fig. 5c), this type of IPyC fracture was more common than the type shown in Fig. 5e. Subsequent analysis of particles with failed SiC layers (discussed in the next section) revealed that most exhibited buffer-induced IPyC fracture like that shown in Fig. 5e or Fig. 5f. An important conclusion from this analysis is that low-stress buffer-IPyC debonding appears to be a desirable condition, and fuel properties should be optimized to the extent possible to produce this end result.

No significant dependence of particle morphology on burnup, fast fluence, or temperature was apparent over the range of irradiation conditions represented by the compacts examined in the AGR-1 PIE. After safety testing, similar particle morphologies were generally observed, although instances of SiC failure increased (see Section IV).

IV. COATING FAILURE ANALYSIS

Particles that experienced SiC layer failure during irradiation or during safety tests were identified based on elevated cesium release, and many of these were analyzed in detail both nondestructively, using x-ray imaging with tomographic reconstruction, and by cross sectioning and microanalysis using a number of analytical characterization methods.^{11,18} For SiC failures during irradiation, the examination process started with gamma-scanning the empty graphite fuel holders to locate regions with elevated cesium activity. The compacts that were adjacent to these regions during irradiation were then deconsolidated to liberate the particles, which were all gamma counted to quantify the inventory of Cs-137, Cs-134, and Ce-144. Particles that exhibited abnormally low cesium inventory were then collected, and x-ray imaging was used to nondestructively observe the interior particle morphology.

In total, three particles with high cesium release during irradiation were found and examined (a fourth particle was detected during deconsolidation-leach-burn-leach analysis of another compact, but was destroyed in the process). In all of these particles, a similar failure mechanism was implicated. Buffer shrinkage resulted in IPyC fracture due to incomplete debonding at the buffer-IPyC interface. In one case, arrowhead-like fracture occurred (similar to that shown in Fig. 5e), while in the other two particles, IPyC fracture was related to stress from the buffer pulling away from the IPyC (similar to Fig 5f). The IPyC fracture then exposed the SiC layer to concentrated chemical attack of

fission products (notably palladium), which caused degradation through the entire layer (Fig. 6). It is noteworthy that significant attack of the SiC layer was never observed in particles without this sort of IPyC fracture, nor in these three particles in areas away from the IPyC fracture. So while these failures were ultimately precipitated by Pd attack on SiC, prior fracture of the IPyC layer appears to be a prerequisite for the attack to occur.

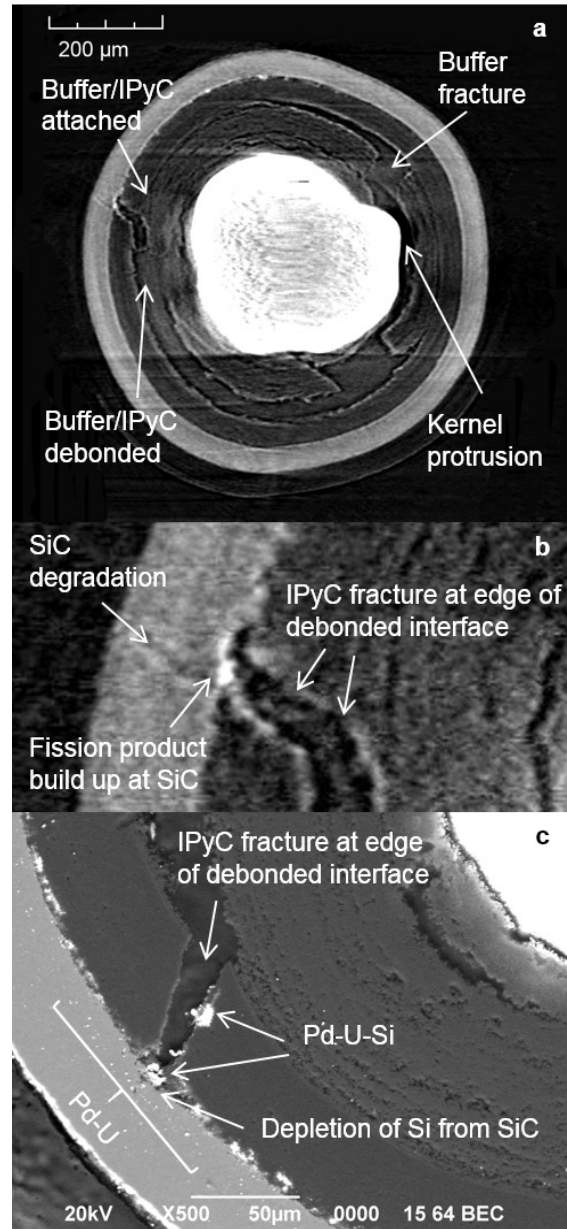


Fig. 6. (a) X-ray tomogram showing microstructure in an irradiated Compact 5-2-3 particle that led to SiC failure and cesium release; (b) x-ray closeup of degraded pathway through SiC; and (c) SEM micrograph of degraded region with EDS identification of Pd and U in the SiC and Si outside the SiC.

Safety testing produced SiC failures in fractions higher than during irradiation, with the failure fraction increasing with test temperature. At 1600°C, two of the three particles with SiC failures that were identified were examined in detail, and the cause of the SiC failure was determined to be an as-fabricated defect in the SiC layer¹⁸ (the third particle was not recovered for analysis). At 1700 and 1800°C, nearly all of the particles recovered exhibited a similar SiC failure mechanism to the one identified for the as-irradiated particles. The major differences were that the elevated temperature increased the severity of the SiC degradation due to enhanced reaction with fission products (Fig. 7). The total SiC layer failure fractions during irradiation and during safety testing are presented in Table 2 as absolute failure fraction in the analyzed compacts and the maximum fraction that might be observed in the entire lot of AGR-1 test fuel, calculated statistically at the 95% confidence level.¹¹

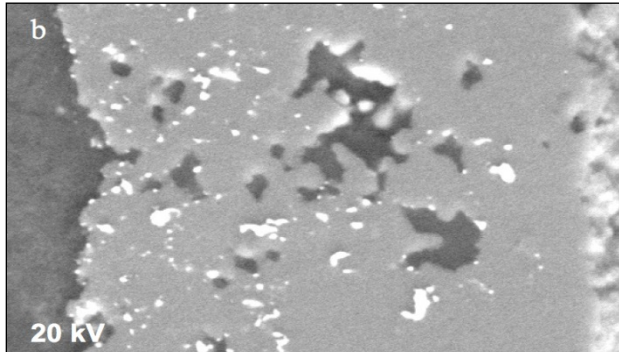


Fig. 7. SiC layer of an irradiated particle that was heated at 1700°C for 300 h, showing the specific area in the SiC that was corroded by focused attack of Pd due to IPyC fracture. From Ref. 11.

The dominant SiC failure mechanism described here is significantly different from that currently embedded in fuel performance models, including the code PARFUME.²⁶ Insertion of this failure mode into the models is likely to be challenging due to its complex nature (essentially a two-part mechanism, involving thermomechanical behavior of the buffer and IPyC under irradiation, and focused chemical attack of the SiC layer) and a lack of some key data (including buffer strength, buffer-IPyC bond strength, fission product partitioning coefficients at the site of the IPyC fracture, and reaction kinetics for the chemical degradation). The nature of the SiC failures, including their correlation with buffer-IPyC delamination, suggests that a reduction in effective bond strength between the buffer and IPyC layers would be desirable from a fabrication standpoint. Qualitative data suggests that this bond strength is lower in the AGR-2 fuel than in the AGR-1 fuel. PIE and safety testing of the AGR-2 fuel is currently underway,^{23,24} and an important observation will be the relative incidence of buffer-IPyC delamination and SiC failures by this mechanism relative to AGR-1.

As discussed above in the context of krypton release, no TRISO failures were observed during the irradiation or during safety testing at 1600 and 1700°C, while two TRISO failures were observed during testing at 1800°C. The resulting failure fractions (absolute failure fraction and failure fraction at 95% confidence) are shown in Table 2. Note that if the 1600 and 1700°C failure statistics from Table 2 are combined, the resulting TRISO failure fractions at 95% confidence for normal operation and during accidents are lower than available reactor design specifications by a factor of at least 9 (see Table 3).

Table 2. Summary of SiC and TRISO failure fractions in AGR-1 fuel during irradiation and safety testing.

Particle Conditions	Number of Particles Tested ¹ (Number of compacts tested)	SiC Failures			TRISO Failures		
		Number of Failures	Failure Fraction		Number of Failures	Failure Fraction	
			Measured	95% Confidence		Measured	95% Confidence
As-irradiated	298,000 (72)	4	1.3×10^{-5}	$\leq 3.1 \times 10^{-5}$	0	0	$\leq 1.1 \times 10^{-5}$
1600°C safety-tested	33,100 (8)	3	9.1×10^{-5}	$\leq 2.4 \times 10^{-4}$	0	0	$\leq 9.1 \times 10^{-5}$
1700°C safety-tested	12,400 (3)	7	5.6×10^{-4}	$\leq 1.1 \times 10^{-3}$	0	0	$\leq 2.5 \times 10^{-4}$
1800°C safety-tested	16,500 (4)	23	1.4×10^{-3}	$\leq 2.0 \times 10^{-3}$	2	1.2×10^{-4}	$\leq 3.9 \times 10^{-4}$

¹ Particle numbers are approximate and are based on the average number of particles per compact

Table 3. AGR-1 TRISO failure fractions compared to preliminary US prismatic NGNP and HTR-Modul design specifications.

Condition	Design specifications for particle failure fraction		AGR-1 95% confidence
	NGNP ^a	HTR-Modul ^b	
In-service	$\leq 2.0 \times 10^{-4}$	$\leq 1.6 \times 10^{-4}$	$\leq 1.1 \times 10^{-5}$
1600°C accident	$\leq 6.0 \times 10^{-4}$	$\leq 6.6 \times 10^{-4}$	$\leq 6.6 \times 10^{-5}$ ^c

^a Values from Ref. 27, Table 16

^b Values from Ref. 27, Table 13. “In-service” failure specification corresponds to the value at 1200°C.

^c Value obtained by combining statistics from 1600 and 1700°C AGR-1 safety tests (0 failures out of 45,550 particles)

V. SILVER AND PALLADIUM TRANSPORT

Significant silver release has been noted since the early days of TRISO fuel irradiation testing.^{15,16} However, these observations have been limited to the results of integral tests (i.e., the observation of silver released from TRISO fuel elements during irradiation or during post-irradiation heating tests), and an understanding of the precise mechanism of silver transport has been lacking. In addition, interaction of fission products such as palladium with SiC, resulting in degradation of the layer, has also been a common observation,^{28,29} although transport through the layer has not been studied in detail, and the potential role that palladium might have in silver the transport of other fission products is not well understood. Hence a detailed study of fission products within the SiC microstructure—including silver and palladium—is of great interest.

Several modern analytical tools have become available in recent decades that enable a detailed microstructural characterization of materials, and the increasing availability of such tools for use on irradiated fuel, including sample preparation using the focused ion beam³⁰ (FIB), is making in-depth analysis of irradiated TRISO particles at nanometer length scales feasible. For the irradiated AGR-1 fuel, basic microstructural and elemental analysis has been performed on particle cross sections using scanning electron microscopy (SEM) with integrated elemental analysis.^{11,31} These methods are able to identify fission product inclusions on a relatively gross scale (particle sizes in excess of several micrometers), but additional analysis is needed to characterize the inclusions in detail.

A FIB has been used to prepare lamella from irradiated AGR-1 particle cross sections for further analysis. Characterization techniques include transmission electron microscopy (TEM), scanning transmission electron microscopy (STEM) with energy dispersive spectroscopy (EDS), electron energy loss spectroscopy (EELS), and precession electron diffraction (PED), among others. The

overall goal is to identify specific fission products within the SiC microstructure^{32,33} and, where possible, to correlate the location of fission products with the type of local environment (e.g., type of grain boundaries^{34,35}) and draw conclusions about the nature of fission product transport.

Using SEM-EDS analysis, fission product clusters were observed in particle cross-sections, often collecting at the IPyC-SiC interface, and also within the SiC layer. At this resolution, the dominant fission product observed in the clusters was palladium, often observed together with uranium. Higher resolution analysis with TEM/STEM revealed numerous other fission products along with palladium and uranium in the SiC layer. Among these fission products was silver, which was observed for the first time in irradiated TRISO particle coating layers.³²

Results to date indicate that the specific location of fission products within the SiC microstructure can be diverse (i.e., grain boundaries of different types and misorientation angles, grain boundary triple points, and within SiC grains), and the composition of the fission product inclusions can be complex, including various combinations of fission products and actinides (palladium, silver, uranium, and others). This makes for challenging interpretation of fission product behavior. While microanalytical characterization of the AGR-1 fuel is still in progress, some of the additional pertinent findings with regard to fission product transport in the layers are summarized below.¹¹

- Fission products are almost always located at grain boundaries.
- Silver is usually found in conjunction with other fission products (e.g., palladium), although some examples of isolated silver precipitates (i.e., without other fission products) have been found.
- Very small fission product inclusions (usually on grain boundaries) have been identified throughout the entire thickness of the SiC layer in some particles, even in cases where the SiC layer was not failed and still effectively retained cesium.
- Initial results indicate that fission products favor random, high-angle grain boundaries in the SiC layer.
- Fission product clusters in the SiC are often accompanied by uranium.

Work is ongoing in this area and is expected to continue to enhance our understanding of fission product behavior within TRISO particles. Work has also commenced on microanalysis of AGR-2 fuel

VI. CONCLUSIONS

The AGR-1 irradiation and PIE have demonstrated fuel performance of UCO fuel to nearly 20% FIMA, with fast fluence of up to 4.30×10^{25} n/m² and time-average, volume-average temperatures of up to 1136°C that exceeds

anticipated design criteria. This includes a low incidence of coating failures and low in-pile release of krypton and cesium. Release of europium and strontium through intact coatings was observed, with significant fractions of the released inventory were retained in the compact matrix during irradiation. Safety testing likewise demonstrated excellent fuel behavior, particularly in terms of the TRISO coating failure fractions and the Kr and Cs release fractions.

While AGR-1 was intended as an initial test to gather preliminary data on lab-scale fuel performance, it represents the most extensive irradiation, PIE, and safety testing database yet reported for UCO fuel, and the results are promising. Subsequent irradiation tests, including AGR-2 (PIE currently in progress) and AGR-5/6/7 (irradiation scheduled to start in 2017), will demonstrate performance characteristics of fuel fabricated at the engineering scale.

ACKNOWLEDGMENTS

This work was supported by the U.S. Department of Energy, Office of Nuclear Energy. The authors wish to thank the many members of the excellent technical teams at ORNL and INL for their valuable contributions during the AGR-1 PIE. C.A. Baldwin, F.C. Montgomery, and T.J. Gerczak at ORNL are acknowledged for their help with the compact deconsolidation and particle analysis, and the ORNL Irradiated Fuels Examination Laboratory and Nuclear Analytical Chemistry Laboratory for PIE support and radiochemical analysis. Technical support for irradiation and PIE at INL was provided by S.B. Grover, J.T. Maki, J.M. Harp, P.L. Winston, S.A. Ploger, I.J. van Rooyen and the advanced microscopy team, as well as the staff at the Hot Fuel Examination Facility, the Analytical Laboratory, and the Electron Microscopy Laboratory.

REFERENCES

1. D.A. PETTI, J.T. MAKI, J.D. HUNN, P.J. PAPPANO, C.M. BARNES, J.J. SAURWEIN, S.G. NAGLEY, J.M. KENDALL, and R.R. HOBBINS, "The DOE Advanced Gas Reactor Fuel Development and Qualification Program," *JOM*, **62**, 62–66 (2010).
2. J.A. PHILIPS, C.M. BARNES, J.D. HUNN, "Fabrication and comparison of fuels for Advanced Gas Reactor irradiation tests," *Proceedings of HTR2010*, Prague, Czech Republic, 18–20 Oct. 2010, Paper 236.
3. P.J. PAPPANO, T.D. BURCHELL, J.D. HUNN, M.P. TRAMMELL, "A novel approach to fabricating fuel compacts for the Next Generation Nuclear Plant (NGNP)," *Journal of Nuclear Materials*, **381** 25 (2008).
4. R.A. LOWDEN, *Fabrication of Baseline and Variant Particle Fuel for AGR-1*, ORNL/CF-06/02, Oak Ridge National Laboratory, 2006.
5. J.D. HUNN, G.E. JELLISON Jr., R.A. LOWDEN, Increase in pyrolytic carbon optical anisotropy and density during processing of coated particle fuel due to heat treatment, *Journal of Nuclear Materials*, **374**, 445-452 (2007).
6. T.J. GERCZAK, J.D. HUNN, R.A. LOWDER, T.R. ALLEN, "SiC layer microstructure in AGR-1 and AGR-2 TRISO fuel particles and the influence of its variation on the effective diffusion of key fission products," *Journal of Nuclear Materials*, **480**, 1–14 (2016).
7. J.D. HUNN, T.W. SAVAGE, J.S. KEHN, AGR-1 Fuel Compact Pre-Irradiation Characterization Summary Report, ORNL/TM-2012/295, Oak Ridge National Laboratory, 2012.
8. S.B. GROVER, D.A. PETTI, J.T. MAKI, "Completion of the first NGNP advanced gas reactor fuel irradiation experiment, AGR-1, in the advanced test reactor," *Proceedings of HT2010*, Prague, Czech Republic, October 18-20, 2010, Paper 104.
9. B.P. COLLIN, AGR-1 Irradiation Test Final As-Run Report, INL/EXT-10-18097 Revision 3, Idaho National Laboratory, 2015.
10. R.N. MORRIS, C. A. BALDWIN, P. A. DEMKOWICZ, J. D. HUNN, and E. L. REBER, Performance of AGR-1 high-temperature reactor fuel during post-irradiation heating tests," *Nuclear Engineering and Design*, **306**, 24-35 (2016).
11. P.A. DEMKOWICZ, J.D. HUNN, R.N. MORRIS, I. VAN ROOYEN, T. GERCZAK, J.M. HARP, S.A. PLOGER, "AGR-1 Post-Irradiation Examination Final Report," INL/EXT-15-36407, Idaho National Laboratory, 2015.
12. P.A. DEMKOWICZ, E.L. REBER, D.M. SCATES, L. SCOTT, "First high temperature safety tests of AGR 1 TRISO fuel with the Fuel Accident Condition Simulator (FACS) furnace," *Journal of Nuclear Materials*, **464**, 320-330 (2015).
13. P.A. DEMKOWICZ, J.D. HUNN, S.A. PLOGER, R.N. MORRIS, C.A. BALDWIN, J.M. HARP, P.L. WINSTON, T.J. GERCZAK, I.J. VAN ROOYEN, F.C. MONTGOMERY, C.M. SILVA, "Irradiation performance of AGR-1 high temperature reactor fuel," *Nuclear Engineering and Design*, **306**, 2-13 (2016).
14. J.D. HUNN, T.J. GERCZAK, R.N. MORRIS, C.A. BALDWIN, F. C. MONTGOMERY, *PIE on Safety-Tested Loose Particles from AGR-1 Compact 4-4-2*, ORNL/TM-2015/161, Oak Ridge National Laboratory, 2016.
15. H. NABIELEK, P.E. BROWN, P. OFFERMAN, *Nuclear Technology*, **35**, 483-493 (1977).
16. W. AMIAN, D. STÖVER, *Nuclear Technology* **61**, 475-486 (1983).

17. G.L. Hawkes, "AGR-1 Daily As-Run Thermal Analyses," ECAR-968 Revision 3, Idaho National Laboratory, 2014.

18. J.D. HUNN, C.A. BALDWIN, T.J. GERCZAK, F. C. MONTGOMERY, R.N. MORRIS, C.M. SILVA, P.A. DEMKOWICZ, J.M. HARP, S.A. PLOGER, "Detection and analysis of particles with failed SiC in AGR-1 fuel compacts," *Nuclear Engineering and Design*, **306**, 36-46 (2016).

19. P.A. DEMKOWICZ, J.M. HARP, P.L. WINSTON, and S.A. PLOGER, Analysis of Fission Products on the AGR 1 Capsule Components, INL/EXT 13 28483, Rev. 0, Idaho National Laboratory, 2013.

20. H. HANTKE, "Performance of High Quality HTR LEU Fuel Elements with TRISO Coated Particles," Forschungszentrum Jülich Internal Report HTA-IB-7/92, 1992.

21. D. FREIS, P.D.W. BOTTOMLEY, A.I. KELLERBAUER, V.V. RRONDINELLA, and P. VAN UFFELEN, "Accident testing of high-temperature reactor fuel elements from the HFR-EU1bis irradiation," *Nuclear Engineering and Design*, **241**, 2813-2821 (2011).

22. O. SEEGER, M. LAURIE, A. EL ABJANI, J. ETJON, D. BOUDAUD, D. FREIS, P. CARBOL, V.V. RONDINELLA, M. FÜTTERER, and H.J. ALLELEIN, "KüFA Safety Testing of HTR Fuel Pebbles irradiated in the High Flux Reactor in Petten," *Proceedings HTR-2014*, October 27-31, 2014, Weihai, China, Paper HTR2014-31149.

23. J.D. HUNN, C.A. BALDWIN, F.C. MONTGOMERY, T.J. GERCZAK, R.N. MORRIS, G.W. HELMREICH, P.A. DEMKOWICZ, J.M. HARP, J.D. STEMPIEN, "Initial examination of fuel compacts and TRISO particles from the US AGR-2 irradiation test," *Proceedings of HTR2016*, Las Vegas, Nevada, USA, November 6-10 2016, Paper 18443.

24. R.N. MORRIS, J.D. HUNN, C.A. BALDWIN, F.C. MONTGOMERY, TYLER GERCZAK, P.A. DEMKOWICZ, "Initial results from safety testing of US AGR-2 irradiation test fuel," *Proceedings of HTR2016*, Las Vegas, Nevada, USA, November 6-10 2016, Paper 18574.

25. S.A. PLOGER, P.A. DEMKOWICZ, J.D. HUNN, J.S. KEHN, "Microscopic analysis of irradiated AGR-1 coated particle fuel compacts," *Nuclear Engineering and Design*, **271**, 221-230 (2014).

26. B.P. COLLIN, D.A. PETTI, P.A. DEMKOWICZ, J.T. MAKI, "Comparison of silver, cesium, and strontium release predictions using PARFUME with results from the AGR-1 irradiation experiments," *Journal of Nuclear Materials*, **466**, 426-442 (2015).

27. NGNP Fuel Qualification White Paper, INL/EXT-10-18610, Idaho National Laboratory, 2010.

28. K. MINATO, T. OGAWA, S. KASHIMURA, K. FUKUDA, M. SHIMIZU, Y. TAYAMA, I. TAKAHASHI, "Fission-product palladium silicon-carbide interaction in HTGR fuel-particles," *Journal of Nuclear Materials*, **172**, 184-196 (1990).

29. K. MINATO, T. OGAWA, K. FUKUDA, M. SHIMIZU, Y. TAYAMA, I. TAKAHASHI, "Fission-product behavior in TRISO-coated UO₂ fuel-particles," *Journal of Nuclear Materials*, **208**, 266-281 (1994).

30. B.D. MILLER, J. GAN, J. MADDEN, J.F. JUE, A. ROBINSON, D.D. KEISER JR., "Advantages and disadvantages of using a focused ion beam to prepare TEM samples from irradiated U-10Mo monolithic nuclear fuel," *Journal of Nuclear Materials*, **424**, 38-42 (2012).

31. I.J. VAN ROOYEN, D.E. JANNEY, B.D. MILLER, P.A. DEMKOWICZ, and J. RIESTERER, "Electron microscopic evaluation and fission product identification of irradiated TRISO coated particles from the AGR-1 experiment: A preliminary review," *Nuclear Engineering and Design*, **271**, 114-122 (2014).

32. I.J. VAN ROOYEN, T.M. LILLO, Y.Q. WU, "Identification of silver and palladium in irradiated TRISO coated particles of the AGR-1 experiment," *Journal of Nuclear Materials*, **446**, 178-186 (2014).

33. T.M. LILLO, I.J. VAN ROOYEN, "Associations of Pd, U and Ag in the SiC layer of neutron-irradiated TRISO fuel," *Journal of Nuclear Materials*, **460**, 97-106 (2015).

34. T.M. LILLO, I.J. VAN ROOYEN, Influence of SiC grain boundary character on fission product transport in irradiated TRISO fuel," *Journal of Nuclear Materials*, **473**, 83-92 (2016).

35. T.M. LILLO, I.J. VAN ROOYEN, J.A. AGUIAR, "Silicon carbide grain boundary distributions, irradiation conditions, and silver retention in irradiated AGR-1 TRISO fuel particles," *Proceedings of HTR2016*, Las Vegas, Nevada, USA, November 6-10 2016, Paper 18560.